International Journal of Innovative
Computing, Information and Control
Volume **18**, Number **5**, October **2022**

ICIC International ©2022 ISSN 1349-4198
pp. **1519–1536**

DISSIPATIVE ANALYSIS AND EVENT-TRIGGERED EXPONENTIAL SYNCHRONIZATION FOR FRACTIONAL-ORDER COMPLEX-VALUED REACTION-DIFFUSION NEURAL NETWORKS

Xiangliang Sun and Xiaona Song*

School of Information Engineering
Henan University of Science and Technology
No. 263, Kaiyuan Avenue, Luolong District, Luoyang 471000, P. R. China
200320050429@haust.stu.edu.cn; *Corresponding author: xiaona97@haust.edu.cn

Received December 2021; revised April 2022

Abstract. *This paper considers the dissipative analysis and exponential synchronization for a class of fractional-order complex-valued neural networks with reaction-diffusion terms. First, the dissipativity of the constructed system is proved by using the fractional Halanay inequality. In addition, to reduce the frequency of information exchange between the controller and the system, a unique event-triggered mechanism is employed to guarantee that the criterion of exponential synchronization holds. Furthermore, a positive lower bound of the event-triggered interval is calculated to avoid the Zeno behavior. Finally, two numerical examples are provided to illustrate the feasibility of the results in this paper.*

Keywords: Fractional-order, Complex-valued neural networks, Exponential synchronization, Reaction-diffusion terms, Event-triggered mechanism, Dissipativity

1. **Introduction.** Neural networks (NNs) are hot topic that have been widely used in image encryption [1], state estimation [2], information processing [3] and so on [4-10]. In recent years, some phenomena in memory processes and fractal structures have been found to be closely related to fractional calculus. Therefore, scholars have tried to introduce fractional order into NNs to build a more comprehensive model, for instance, [11] improved the capacitance of integer-order NNs to obtain fractional-order neural networks (FONNs), which enabled the properties of fractional order can be represented in NNs. Compared with the integer calculus, the advantage of fractional-order derivative is that it's nonlocal and has weak singular kernels. Furthermore, studies have shown that fractional-order differential equations have infinite memory and more degrees of freedom. Therefore, many fruitful studies involving FONNs have been presented. For example, in [12], the authors studied fractional-order memristor-based NNs and given the projective synchronization criteria for the proposed system; the finite-time stability for fractional-order NNs with delay has been discussed in [13]; in [14], the authors analyzed the asymptotic stability of delayed fractional-order NNs with impulsive effects.

In practice, all physical processes have spatial distribution characteristics, such as chemical processes, biological systems, and electromagnetic fields. However, traditional NNs ignore the influence of spatial factors on neurons, which is inconsistent with some actual phenomena [15, 16]. In addition, the reaction-diffusion phenomenon has to be considered when we study the movement of electrons in the magnetic field. Therefore, it is significant to consider the reaction-diffusion terms on NNs [17]. Many innovative works have published by predecessors. For instance, in [18], the finite-time synchronization criteria

DOI: 10.24507/ijicic.18.05.1519

for reaction-diffusion inertial memristive NNs have been obtained via gain-scheduled pinning control; for stochastic delay reaction-diffusion NNs, the exponential input-to-state stability has been investigated in [19].

It is worth noting that the above studies are all based on the real domain; however, the results show that the complex-valued neural networks (CVNNs) have more advantages in data processing compared to real-valued ones [20, 21]. Most importantly, it can solve the XOR problem that the real domain cannot solve [22]. Naturally, the above descriptions raise a question for us: can the existing fractional-order reaction-diffusion NNs be extended to complex domains? Unfortunately, to the best of authors' knowledge, there is less research on this question which inspired us to construct a model of fractional-order complex-valued neural networks (FOCVNNs) with reaction-diffusion terms, and investigate it is dynamical behaviour.

The dynamic analysis of NNs has always been a hot topic, including stability analysis, dissipative analysis, synchronization analysis, etc. Synchronization is the convergence of the states for multiple systems under the action of external factors, and there are many researches in the published papers, for example, for a class of discontinuous NNs, the synchronization criteria were obtained via functional differential inclusions in [23]; for FONNs, the projective synchronization was investigated in [24]. Dissipative theory, first proposed in 1972 [25], is mainly used to describe the energy decay of a system; in other words, the system will eventually converge to a dissipative set over time. In general, dissipativity provides more information than stability, which is strictly combined with the phenomenon of loss or dissipation of energy. Hence, dissipation theory provided a new method for systematic analysis and has been extensively studied, for instance, the extended dissipativity for Markov jump NNs was performed in [26]; in [27], event-based extended dissipative for a class of NNs was addressed. While, to the best of our knowledge, until now, there is no dissipative analysis on FOCVNNs with reaction-diffusion terms.

To synchronize NNs, many control methods were proposed, such as impulsive control [28, 29], adaptive control [30, 31], and sliding mode control [24, 32]. It is worth noting that all of the above articles are established on the continuous exchange of information, that will be a higher requirement for communication bandwidth of the system. In fact, it is difficult to guarantee that the signal is continuous and there are limitations on the bandwidth in most systems. Therefore, event-triggered control is used to reduce the frequency of information exchange; furthermore, sampled-data event-triggered control (sampling data first and determining event triggers later) is widely used to avoid Zeno behavior [33, 34]. Inspired by [35], this paper attempts to employ an event-triggered controller without sampled-data, and gives a positive lower bound of the event-triggered interval time.

Based on the above discussions, the dissipative analysis for FOCVNNs with reaction-diffusion terms is first considered in this paper, and then we study the issue of exponential synchronization of the proposed model, where a new event-triggered controller is designed for bandwidth saving. The main contributions are as follows.

1) The fractional order and spatial term have been involved in the CVNNs [36, 37] and [38, 39], respectively. However, a more comprehensive model is still lacking. Inspired by the above literature, this paper attempts to take fractional order and reaction-diffusion terms into account simultaneously to construct FOCVNNs with reaction-diffusion terms, which means the model of this paper is more comprehensive. In addition, the new model is proved to be dissipative via fractional Halanay inequality.

2) To relieve the stress of communication, [35] designed event-triggered controllers to guarantee the exponential synchronization for CVNNs; event-triggered synchronization for reaction-diffusion NNs was studied in [40]. However, there is a lack of event-triggered

control for CVNNs which involve both fractional order and spatial terms. In this paper, a unique event-triggered controller is proposed for the first time to ensure that FOCVNNs with reaction-diffusion terms can achieve exponential synchronization.

3) In most of the event-triggered control schemes, the time term is usually divided first and then the data is collected at the sampling point [33, 41], which can avoid the Zeno behavior but it may lose some key data. Instead of the above approach, in [35], the authors used a new event-triggered mechanism to derive a positive lower bound of the trigger time interval to ensure that Zeno behaviour does not occur. Inspired by this method, we designed a novel event-triggered scheme to make the FOCVNNs with reaction-diffusion terms achieve exponential synchronization and obtain the positive lower bound for the event-triggered time interval by using the fractional calculus theorem.

The remainder of this paper is organized as follows. First, abbreviations for some letters are shown in notations. In Section 2, the necessary lemma and definitions are given, and then the model of FOCVNNs with reaction-diffusion terms is constructed. The dissipative analysis of the proposed model is proved by employing fractional Halanay inequality. In addition, a special event-triggered controller is designed to realize exponential synchronization for the master-slave system; furthermore, the Zeno behavior is avoided in Section 3. To verify the results, two examples are provided in Section 4. Finally, we conclude this paper in Section 5.

To present the main contributions more clearly, a comparison with other articles was given in Table 1. In addition, dissipative analysis, exponential synchronization, fractional order, reaction-diffusion terms, complex valued and event-triggered mechanism are replaced by DA, ES, FO, RD, CV and ETM, respectively; $\surd$ means this item is included in that paper, and $\times$ means it is not.

Table 1. Comparison with other papers

NNs	[35]	[36]	[37]	[38]	[40]	This paper
DA	$\times$	$\times$	$\surd$	$\times$	$\times$	$\surd$
ES	$\surd$	$\times$	$\times$	$\times$	$\times$	$\surd$
FO	$\times$	$\surd$	$\surd$	$\times$	$\times$	$\surd$
RD	$\times$	$\times$	$\times$	$\surd$	$\surd$	$\surd$
CV	$\surd$	$\surd$	$\surd$	$\surd$	$\times$	$\surd$
ETM	$\surd$	$\times$	$\times$	$\times$	$\surd$	$\surd$

Notations: Throughout this paper, $|\cdot|$ denotes the modulus of vector; $\|\varrho\|_1 = \sum_{i=1}^{N}|\varrho_i|$, $\|\varrho\|_2 = \sqrt{\sum_{i=1}^{N}\varrho_i^2}$, where ϱ denotes the N-dimensional vectors; $\mathbb{R}^n$ and $\mathbb{C}^n$ represent the set of n-dimensional real-valued and complex-valued vectors, respectively. For simplicity, some symbols are indicated as the following forms: $\grave{c}_{xy}^{\chi} \in \overline{co}\left[c_{xy}^{\chi}(s_x^{\chi})\right] = \left[c_{xy}^{\chi-}, c_{xy}^{\chi+}\right]$, $\grave{d}_{xy}^{\chi} \in \overline{co}\left[d_{xy}^{\chi}(s_x^{\chi})\right] = \left[d_{xy}^{\chi-}, d_{xy}^{\chi+}\right]$, $\acute{c}_{xy}^{\chi} \in \overline{co}\left[c_{xy}^{\chi}(m_x^{\chi})\right] = \left[c_{xy}^{\chi-}, c_{xy}^{\chi+}\right]$, $\acute{d}_{xy}^{\chi} \in \overline{co}\left[d_{xy}^{\chi}(m_x^{\chi})\right] = \left[d_{xy}^{\chi-}, d_{xy}^{\chi+}\right]$, $c_x^{\chi-} = \min\left\{\dot{c}_{xy}^{\chi}, \ddot{c}_{xy}^{\chi}\right\}$, $c_x^{\chi+} = \max\left\{\dot{c}_{xy}^{\chi}, \ddot{c}_{xy}^{\chi}\right\}$, $d_x^{\chi-} = \min\left\{\dot{d}_{xy}^{\chi}, \ddot{d}_{xy}^{\chi}\right\}$, $d_x^{\chi+} = \max\left\{\dot{d}_{xy}^{\chi}, \ddot{d}_{xy}^{\chi}\right\}$, $\Delta_x^{\chi} = \Delta_x^{\chi}(z,t)$ $(\Delta = s, m, e, V)$, $\varphi_{y\sigma}^{\chi} = \varphi_y^{\chi}(z, t-\sigma(t))$ $(\varphi = s, m, e)$, $u(t_k)_x^{\chi} = u(z,t_k)_x^{\chi}$, where z denotes the spatial position, $\sigma(t)$ is the time-varying delay and $z = (z_1, z_2, \ldots, z_q)^T \in \Omega \subset \mathbb{R}^n$, with $\Omega = \{z||z_k| \le \imath_k, k = 1, 2, \ldots, n\}$ and $\imath_k$ is a positive constant. In addition, $\chi = (I, R)$ shows the real and imaginary parts of the parameter, that means the complex-valued system is considered as a combination of two real-valued systems.

2. Problem Formulation and Preliminaries.

2.1. Necessary lemma and definitions.

Lemma 2.1. *(see [42]) If there exist a real function $h(s)$ and a differentiable real function $\eta(t)$, such that $\S(t)$ satisfies $\S(t) \leq \int_{t_0}^{t} h(s)\S(s)ds + \eta(t)$, then one has*

$$\S(t) \leq \eta(t_0)\exp\left(\int_{t_0}^{t} h(s)ds\right) + \int_{t_0}^{t} \dot{\eta}(s)\exp\left(\int_{t_0}^{t} h(s)ds\right)ds.$$

If $\eta(t) = \eta$, where η denotes a constant, then $\S(t) \leq \eta\exp\left(\int_{t_0}^{t} h(s)ds\right)$.

Definition 2.1. *(see [43]) For the integrable function $K(t)$, its fractional integral with $0 < \alpha < 1$ can be defined as*

$$I^{\alpha}K(t) = \frac{1}{\Gamma(\alpha)}\int_{0}^{t}(t-s)^{\alpha-1}K(s)ds, \tag{1}$$

where the gamma function $\Gamma(\alpha)$ satisfies $\Gamma(\alpha) = \int_{0}^{+\infty} s^{\alpha-1}e^{-s}ds$.

Definition 2.2. *(see [43]) For differentiable function $\wp(t)$, its Caputo fractional derivative is defined as*

$$D^{\alpha}\wp(t) = \frac{1}{\Gamma(i-\alpha)}\int_{t_0}^{t}(t-s)^{i-\alpha-1}\wp^{(i)}(s)ds, \tag{2}$$

where $t \geq t_0$, i is a positive integer, and $\alpha \in (i-1, i)$; especially, when $\alpha \in (0, 1)$,

$$D^{\alpha}\wp(t) = \frac{1}{\Gamma(1-\alpha)}\int_{t_0}^{t}\frac{\wp'(s)}{(t-s)^{\alpha}}ds. \tag{3}$$

Definition 2.3. *(see [37] Definition 4) If there exists a compact set $B \subset \mathbb{C}^n$, such that $\forall s_0 \in \mathbb{C}^n$, $\exists T > 0$, when $t \geq t_0 + T$, $s(t, t_0, s_0) \in B$, the system (4) is said to be a dissipative system, and B is a globally attractive set, where t_0 and s_0 denote the initial time and initial state of the system (4), respectively; $s(t, t_0, s_0)$ represents the solution of system (4).*

Definition 2.4. *[44] If there exist positive constants λ_1 and λ_2 such that the following relationship holds*

$$\|m(z,t) - s(z,t)\|_2 \leq \lambda_1\|\varphi - \phi\|_2 e^{-\lambda_2 t}, \quad t > 0,$$

then error systems (19) and (20) are exponential synchronization.

2.2. Model description.

A class of FOCVNNs with reaction-diffusion terms can be constructed as

$$\frac{\partial^{\alpha}s_x}{\partial t^{\alpha}} = \sum_{\kappa=1}^{q}\frac{\partial}{\partial z_k}\left(a_{xk}\frac{\partial s_x}{\partial z_k}\right) - b_x s_x + \sum_{y=1}^{n} c_{xy}(s_x)g_y(s_y) + \sum_{y=1}^{n} d_{xy}(s_x)g_y(s_{y\sigma}) + O_x, \tag{4}$$

where s_x is the state variable of the xth neuron, where $x \in 1, 2, \ldots, n$; $a_{xk} > 0$ is the transmission diffusion operator; $b_x > 0$ is a given positive feedback coefficient; c_{xy} and d_{xy} denote connection coefficients; $g_y(\cdot) \in \mathbb{C}$ is activation function and O_x is external disturbance on the xth neuron.

Considering the characteristics of CVNNs, it is important to note that $s_x = s_x^R + is_x^I$, $c_{xy}(s_x) = c_{xy}^R\left(s_x^R\right) + ic_{xy}^I\left(s_x^I\right)$, $d_{xy}(s_x) = d_{xy}^R\left(s_x^R\right) + id_{xy}^I\left(s_x^I\right)$, $g_y(s_y) = g_y^R + ig_y^I$, $g_{y\sigma}(s_{y\sigma}) = g_{y\sigma}^R + ig_{y\sigma}^I$, $O_x = O_x^R + O_x^I$. Moreover, $c_{xy}(s_x)$ and $d_{xy}(s_x)$ are switchable parameters that obey the following switching rules:

$$\begin{cases} c_{xy}^{\chi}\left(s_x^{\chi}\right)=\dot{c}_{xy}^{\chi},\ d_{xy}^{\chi}\left(s_x^{\chi}\right)=\dot{d}_{xy}^{\chi}, & \left|s_x^{\chi}\right|\le\Upsilon_x^{\chi}, \\ c_{xy}^{\chi}\left(s_x^{\chi}\right)=\ddot{c}_{xy}^{\chi},\ d_{xy}^{\chi}\left(s_x^{\chi}\right)=\ddot{d}_{xy}^{\chi}, & \left|s_x^{\chi}\right|>\Upsilon_x^{\chi}, \end{cases}$$

where $\chi=(I/R)$, $\dot{c}_{xy}^{\chi}$, $\ddot{c}_{xy}^{\chi}$, $\dot{d}_{xy}^{\chi}$, $\ddot{d}_{xy}^{\chi}$ and $\Upsilon_x^{\chi}>0$ are different given constants.

The boundary and initial conditions for (4) are given as

$$s_x^{\chi}(z,t)=0,\ (z,t)\in\partial\Omega\times[-\sigma_2,+\infty),\quad s_x^{\chi}(z,0)=\phi_x^{\chi}(z,0),\ (z,0)\in\Omega\times[-\sigma_2,0],$$

where $\phi_x^{\chi}(z,0)$ is a continuous and bounded function.

Assumption 2.1. *(see [35]) Let the activation function $g_y^{\chi}(\cdot)$ satisfy*

$$\left|g_y^{\chi}(\cdot)\right|\le G_y^{\chi},\quad \sup\left|g_y^{\chi}\left(o_1\right)-g_y^{\chi}\left(o_2\right)\right|\le l_y^{\chi}\left|o_1-o_2\right|,$$

where l_y^{χ} is a non-negative constants and $o_1\neq o_2$, where o_1 and o_2 are arbitrary constants.

Based on the above analysis, (4) can be divided into real and imaginary parts, that

$$\begin{aligned}\frac{\partial^{\alpha}s_x^R}{\partial t^{\alpha}}=&\sum_{k=1}^{q}\frac{\partial}{\partial z_k}\left(a_{xk}\frac{\partial s_x^R}{\partial z_k}\right)-b_x s_x^R+O_x^R+\sum_{y=1}^{n}c_{xy}^R\left(s_x^R\right)g_y^R\left(s_y^R\right)-\sum_{y=1}^{n}c_{xy}^I\left(s_x^I\right)g_y^I\left(s_y^I\right)\\&+\sum_{y=1}^{n}d_{xy}^R\left(s_x^R\right)g_y^R\left(s_{y\sigma}^R\right)-\sum_{y=1}^{n}d_{xy}^I\left(s_x^I\right)g_y^I\left(s_{y\sigma}^I\right),\end{aligned}\tag{5}$$

and

$$\begin{aligned}\frac{\partial^{\alpha}s_x^I}{\partial t^{\alpha}}=&\sum_{k=1}^{q}\frac{\partial}{\partial z_k}\left(a_{xk}\frac{\partial s_x^I}{\partial z_k}\right)-b_x s_x^I+O_x^I+\sum_{y=1}^{n}c_{xy}^R\left(s_x^R\right)g_y^I\left(s_y^I\right)+\sum_{y=1}^{n}c_{xy}^I\left(s_x^I\right)g_y^R\left(s_y^R\right)\\&+\sum_{y=1}^{n}d_{xy}^R\left(s_x^R\right)g_y^I\left(s_{y\sigma}^I\right)+\sum_{y=1}^{n}d_{xy}^I\left(s_x^I\right)g_y^R\left(s_{y\sigma}^R\right).\end{aligned}\tag{6}$$

3. **Main Results.** In this section, firstly, we investigate the dissipativity of system (4). Additionally, some sufficient conditions for event-triggered exponential synchronization of master-slave systems is given; finally, Zeno behavior proved to be avoidable.

3.1. **Dissipative analysis.** In this paper, a more generalized model is obtained by introducing reaction-diffusion terms into FOCVNNs; furthermore, to investigate the dissipativity of that ones, some sufficient conditions will be derived in Theorem 3.1 via fractional Halanay inequality.

Theorem 3.1. *Let Assumption 2.1 hold, if $M+N<0$, $W>0$, then the system (4) is globally dissipative, and the ball $B\left(0,\sqrt{-\frac{W}{M+N}}+\varepsilon\right)$ is a globally attractive set for any given $\varepsilon>0$, where $M=\max_{1\le x\le n}\{M_1,M_2\}$, $N=\max_{1\le x\le n}\{N_1,N_2\}$,*

$$\begin{aligned}M_1=&\sum_{y=1}^{n}\left(1-\sum_{k=1}^{q}\frac{a_{xk}}{\iota_k^2}-b_x+\left|c_{xy}^{R+}\right|l_y^I+\left|c_{yx}^{R+}\right|l_x^I+\left|d_{xy}^{R+}\right|l_y^I+\left|c_{xy}^{I+}\right|l_y^R+\left|d_{xy}^{I+}\right|l_y^R\right.\\&\left.+\left|c_{yx}^{I+}\right|l_x^I\right),\end{aligned}\tag{7}$$

$$\begin{aligned}M_2=&\sum_{y=1}^{n}\left(1-\sum_{k=1}^{q}\frac{a_{xk}}{\iota_k^2}-b_x+\left|c_{xy}^{R+}\right|l_y^R+\left|c_{yx}^{R+}\right|l_x^R+\left|d_{xy}^{R+}\right|l_y^R+\left|c_{xy}^{I+}\right|l_y^I+\left|d_{xy}^{I+}\right|l_y^I\right.\\&\left.+\left|c_{yx}^{I+}\right|l_x^R\right),\end{aligned}\tag{8}$$

$$N_1 = \sum_{y=1}^{n} \left(\left| d_{xy}^{R+} \right| l_y^I + \left(\left| d_{yx}^{I+} \right| l_x^I \right) \right), \tag{9}$$

$$N_2 = \sum_{y=1}^{n} \left(\left| d_{yx}^{I+} \right| l_x^R + \left(\left| d_{xy}^{R+} \right| l_y^R \right) \right), \tag{10}$$

$$W = \sum_{x=1}^{n} \left(\left(O_x^I \right)^2 + \left(O_x^R \right)^2 \right). \tag{11}$$

Proof: We choose the following Lyapunov functional:

$$V_1 = {V_1}^R + {V_1}^I = \int_\Omega \sum_{x=1}^{n} \left(\left(s_x^R \right)^2 + \left(s_x^I \right)^2 \right) dz.$$

Taking the α-order derivative of ${V_1}^R(t)$ along the trajectories of (5), one has

$$\begin{aligned} D^\alpha {V_1}^R \leq\ & 2 \int_\Omega \sum_{x=1}^{n} s_x^R \left[\sum_{k=1}^{q} \frac{\partial}{\partial z_k} \left(a_{xk} \frac{\partial s_x^R}{\partial z_k} \right) - b_x s_x^R dz + \sum_{y=1}^{n} c_{xy}^R \left(s_x^R \right) g_y^R \left(s_y^R \right) + O_x^R \right. \\ & \left. + \sum_{y=1}^{n} d_{xy}^R \left(s_x^R \right) g_y^R \left(s_{y\sigma}^R \right) - \sum_{y=1}^{n} c_{xy}^I \left(s_x^I \right) g_y^I \left(s_y^I \right) - \sum_{y=1}^{n} d_{xy}^I \left(s_x^I \right) g_y^I \left(s_{y\sigma}^I \right) \right] dz. \end{aligned} \tag{12}$$

Next, the terms in (12) need to be processed. It follows from Lemma 1 in [45] and the boundary conditions that

$$\int_\Omega \sum_{x=1}^{n} s_x^R \sum_{k=1}^{q} \frac{\partial}{\partial z_k} \left(a_{xk} \frac{\partial s_x^R}{\partial z_k} \right) dz \leq - \int_\Omega \sum_{x=1}^{n} \sum_{k=1}^{q} \frac{a_{xk}}{\imath_k^2} \left(s_x^R \right)^2 dz. \tag{13}$$

Using Assumption 2.1, one has

$$\begin{aligned} & 2 \int_\Omega \sum_{x=1}^{n} s_x^R \sum_{y=1}^{n} c_{xy}^\chi \left(s_x^\chi \right) g_y^\chi \left(s_y^\chi \right) dz \leq \int_\Omega \sum_{x=1}^{n} \sum_{y=1}^{n} \left(\left| c_{xy}^{\chi+} \right| l_y^\chi \left(s_x^R \right)^2 + \left| c_{yx}^{\chi+} \right| l_x^\chi \left(s_x^\chi \right)^2 \right) dz, \\ & 2 \int_\Omega \sum_{x=1}^{n} s_x^R \sum_{y=1}^{n} d_{xy}^\chi \left(s_x^\chi \right) g_y^\chi \left(s_{y\sigma}^\chi \right) dz \leq \int_\Omega \sum_{x=1}^{n} \sum_{y=1}^{n} \left(\left| d_{xy}^{\chi+} \right| l_y^\chi \left(s_x^R \right)^2 + \left| d_{yx}^{\chi+} \right| l_x^\chi \left(s_{x\sigma}^\chi \right)^2 \right) dz, \\ & 2 \int_\Omega \sum_{x=1}^{n} s_x^R O_x^R dz \leq \int_\Omega \sum_{x=1}^{n} \left(s_x^R \right)^2 + \left(O_x^R \right)^2 dz. \end{aligned} \tag{14}$$

To this end, (12) can be rewritten as

$$\begin{aligned} D^\alpha {V_1}^R \leq & \int_\Omega \sum_{x=1}^{n} \sum_{y=1}^{n} \left[\left(\left| d_{xy}^{R+} \right| l_y^R \right) \left(s_{x\sigma}^R \right)^2 - \left(\left| c_{yx}^{I+} \right| l_x^I \right) \left(s_x^I \right)^2 - \left(\left| d_{yx}^{I+} \right| l_x^I \right) \left(s_{x\sigma}^I \right)^2 + \left(O_x^R \right)^2 \right] dz \\ & + \int_\Omega \sum_{x=1}^{n} \sum_{y=1}^{n} \left[1 - \sum_{k=1}^{q} \frac{a_{xk}}{\imath_k^2} + \left| c_{xy}^{R+} \right| l_y^R + \left| c_{yx}^{R+} \right| l_x^R - b_x + \left| d_{xy}^{R+} \right| l_y^R - \left| c_{xy}^{I+} \right| l_y^I \right. \\ & \left. - \left| d_{xy}^{I+} \right| l_y^I \right] \left(s_x^R \right)^2 dz. \end{aligned} \tag{15}$$

Throughout similar calculations, $D^\alpha {V_1}^I$ can be computed, and then, invoking $D^\alpha {V_1}^R$ and $D^\alpha {V_1}^I$ yields

$$D^{\alpha}V_1 = \int_{\Omega}\sum_{x=1}^{n}\sum_{y=1}^{n}\Bigg[1-\sum_{k=1}^{q}\frac{a_{xk}}{\imath_k^2}-b_x+\left|c_{xy}^{R+}\right|l_y^I+\left|c_{yx}^{R+}\right|l_x^I+\left|d_{xy}^{R+}\right|l_y^I+\left|c_{xy}^{I+}\right|l_y^R+\left|d_{xy}^{I+}\right|l_y^R$$
$$+\left(\left|c_{yx}^{I+}\right|l_x^I\right)\Bigg]\left(s_x^I\right)^2+\Bigg[1-\sum_{k=1}^{q}\frac{a_{xk}}{\imath_k^2}-b_x+\left|c_{xy}^{R+}\right|l_y^R+\left|c_{yx}^{R+}\right|l_x^R+\left|d_{xy}^{R+}\right|l_y^R+\left|c_{xy}^{I+}\right|l_y^I$$
$$+\left|d_{xy}^{I+}\right|l_y^I+\left(\left|c_{yx}^{I+}\right|l_x^R\right)\Bigg]\left(s_x^R\right)^2+\Big[\left|d_{xy}^{R+}\right|l_y^I+\left(\left|d_{yx}^{I+}\right|l_x^I\right)\Big]\left(s_{x\sigma}^I\right)^2$$
$$+\Big[\left|d_{yx}^{I+}\right|l_x^R+\left(\left|d_{xy}^{R+}\right|l_y^R\right)\Big]\left(s_{x\sigma}^R\right)^2+\int_{\Omega}\sum_{x=1}^{n}\left(\left(O_x^I\right)^2+\left(O_x^R\right)^2\right)dz. \tag{16}$$

Substituting Equations (7)-(11) into (16), we have

$$D^{\alpha}V_1(t,z)\le MV_1(t,z)+NV_1(t-\sigma,z)+W. \tag{17}$$

Using fractional Halanay inequality in [46] Lemma 2.3, then, for any $\varepsilon>0$, the following formula holds:

$$V_1(t,z)\le\varepsilon-\frac{W}{M+N},\quad t\ge\bar{t},$$

where $\bar{t}=\bar{t}(M_0,\varepsilon)$, $M_0=\sup_{t-\sigma\le p\le t}\int_{\Omega}\left\|\phi_x^{\chi}(p,z)\right\|_2^2dz$.

In addition, the ball $B\left(0,\sqrt{-\frac{W}{M+N}}+\varepsilon\right)$ is a globally attractive set of system (4). Thus, the system (4) is globally dissipative. This completes the proof. □

Remark 3.1. *The dissipative theory is widely used in physics and mathematics, and its description of energy input-output provides a new framework for the analysis of systems. Moreover, the storage functions in dissipative theory can be regarded as Lyapunov functions under certain conditions, which means that the dissipative theory can be applied to the study of asymptotic stability, uniqueness of equilibria and so on [47]. Recently, many scholars have made positive contributions to the dissipation analysis of NNs [26,27,37,48], for example, [48] investigated the dissipativity for fractional-order reaction-diffusion NNs; dissipative analysis was performed for FOCVNNs in [37]. Therefore, the study of dissipative analysis is meaningful for the more comprehensive model proposed in this paper.*

3.2. **Event-triggered exponential synchronization control.** To achieve the exponential synchronization, we set system (4) as master system, and the slave system is designed as

$$\frac{\partial^{\alpha}m_x}{\partial t^{\alpha}}=\sum_{\kappa=1}^{q}\frac{\partial}{\partial z_k}\left(a_{xk}\frac{\partial m_x}{\partial z_k}\right)-b_xm_x+\sum_{y=1}^{n}c_{xy}(m_x)g_y(m_y)+\sum_{y=1}^{n}d_{xy}(m_x)g_y(m_{y\sigma})$$
$$+O_x+u_x(t_k), \tag{18}$$

where m_x is the state variable of the xth neuron, and $u_x(t_k)=u_x^R(t_k)+u_x^I(t_k)$ is the controller we designed; the boundary and initial conditions for (18) are

$$m_x^{\chi}(z,t)=0,\ (z,t)\in\partial\Omega\times[-\sigma_2,+\infty),\quad m_x^{\chi}(z,0)=\varphi_x^{\chi}(z,0),\ (z,0)\in\Omega\times[-\sigma_2,0].$$

Obviously, $m_x=m_x^R+im_x^I$, $c_{xy}(m_x)=c_{xy}^R\left(m_x^R\right)+ic_{xy}^I\left(m_x^I\right)$, $d_{xy}(m_x)=d_{xy}^R\left(m_x^R\right)+id_{xy}^I\left(m_x^I\right)$, $g_y(m_y)=g_y^R+ig_y^I$, $g_{y\sigma}(m_{y\sigma})=g_{y\sigma}^R+ig_{y\sigma}^I$, and

$$\begin{cases}c_{xy}^{\chi}\left(m_x^{\chi}\right)=\dot{c}_{xy}^{\chi},\ d_{xy}^{\chi}\left(m_x^{\chi}\right)=\dot{d}_{xy}^{\chi}, & \left|m_x^{\chi}\right|\le\Upsilon_x^{\chi},\\ c_{xy}^{\chi}\left(m_x^{\chi}\right)=\ddot{c}_{xy}^{\chi},\ d_{xy}^{\chi}\left(m_x^{\chi}\right)=\ddot{d}_{xy}^{\chi}, & \left|m_x^{\chi}\right|>\Upsilon_x^{\chi}.\end{cases}$$

Now, we define the synchronization error $e_x^\chi = m_x^\chi - s_x^\chi$, $e_x = e_x^R + ie_x^I$, and denote $\hat{c}_{xy}^\chi = \max\left\{\left|c_{xy}^{\chi-}\right|, \left|c_{xy}^{\chi+}\right|\right\}$, $\tilde{c}_{xy}^\chi = \max\left\{\left|\acute{c}_{xy}^\chi - \grave{c}_{xy}^\chi\right|\right\}$, $\hat{d}_{xy}^\chi = \max\left\{\left|d_{xy}^{\chi-}\right|, \left|d_{xy}^{\chi+}\right|\right\}$, and $\tilde{d}_{xy}^\chi = \max\left\{\left|\acute{d}_{xy}^\chi - \grave{d}_{xy}^\chi\right|\right\}$, and then, we can obtain the error system's real parts:

$$\begin{aligned}\frac{\partial^\alpha e_x^R}{\partial t^\alpha} = &\sum_{k=1}^{q}\frac{\partial}{\partial z_k}\left(a_{xk}\frac{\partial e_x^R}{\partial z_k}\right) + \sum_{y=1}^{n}\Big[\acute{c}_{xy}^R f_y^R\left(e_x^R\right) + \acute{d}_{xy}^R f_y^R\left(e_{y\sigma}^R\right) - \acute{c}_{xy}^I f_y^I\left(e_y^I\right) - \acute{d}_{xy}^I f_y^I\left(e_{y\sigma}^I\right)\\ &-\bar{c}_{xy}^I g_y^I\left(s_y^I\right) - \bar{d}_{xy}^I g_y^I\left(s_{y\sigma}^I\right) + \bar{c}_{xy}^R g_y^R\left(s_y^R\right) + \bar{d}_{xy}^R g_y^R\left(s_{y\sigma}^R\right)\Big] - b_x e_x^R + u(t_k)_x^R. \end{aligned} \tag{19}$$

Moreover, the imaginary one is

$$\begin{aligned}\frac{\partial^\alpha e_x^I}{\partial t^\alpha} = &\sum_{k=1}^{q}\frac{\partial}{\partial z_k}\left(a_{xk}\frac{\partial e_x^I}{\partial z_k}\right) + \sum_{y=1}^{n}\Big[\acute{c}_{xy}^I f_y^R\left(e_y^R\right) + \acute{d}_{xy}^I f_y^R\left(e_{y\sigma}^R\right) + \acute{c}_{xy}^R f_y^I\left(e_y^I\right) + \acute{d}_{xy}^R f_y^I\left(e_{y\sigma}^I\right)\\ &+\bar{c}_{xy}^I g_y^R\left(s_y^R\right) + \bar{d}_{xy}^I g_y^R\left(s_{y\sigma}^R\right) + \bar{c}_{xy}^R g_y^I\left(s_y^I\right) + \bar{d}_{xy}^R g_y^I\left(s_{y\sigma}^I\right)\Big] - b_x e_x^I + u(t_k)_x^I, \end{aligned} \tag{20}$$

where $f_y^\chi\left(e_y^\chi\right) = g_y^\chi\left(m_y^\chi\right) - g_y^\chi\left(s_y^\chi\right)$; $f_y^\chi\left(e_{y\sigma}^\chi\right) = g_y^\chi\left(m_{y\sigma}^\chi\right) - g_y^\chi\left(s_{y\sigma}^\chi\right)$. Let $F_y^\chi = 2G_y^\chi$, obviously, $\left|f_y^\chi(\eta)\right| \le F_y^\chi$.

To reduce the communication bandwidth, the following event-triggered controller is employed:

$$\begin{aligned}&u(t_k)_x^\chi = -\varpi\sum_{y=1}^{n}\left(D_{xy}^R + D_{xy}^I\right)\dot{F}sign(e_x^\chi(t_k)) - \alpha_x^\chi e_x^\chi(t_k) - \beta_x^\chi sign(e_x^\chi(t_k))\\ &t \in [t_k, t_{k+1}), \end{aligned} \tag{21}$$

where $\alpha_x^\chi > 0$ and $\beta_x^\chi \in \mathbb{R}$ are designed controller gains, $\dot{F} = \max\left\{\left|F_y^R\right|, \left|F_y^I\right|\right\}$ and $D_{xy}^\chi = \max\left\{\left|d_{xy}^{\chi-}\right|, \left|d_{xy}^{\chi+}\right|\right\}$; ϖ indicates a plus or minus sign; t_k ($t_0 = 0$) is the instant of signal release which follows the rule:

$$t_{k+1} = \inf\{t > t_k : \Xi > 0\}, \quad k \in \mathbb{N}, \tag{22}$$

where Ξ is the event-triggered function we designed later.

To better describe the event-triggered mechanism, we define $\hat{e}_x^\chi(t) = e_x^\chi(t_k) - e_x^\chi(t)$, $t \in [t_k, t_{k+1})$, and comparison of the system error with $t \in [t_k, t_{k+1})$ to determine whether a trigger occurs.

To obtain exponential stability of the master-slave system, a special event-triggered controller (21) was employed in Theorem 3.2. Furthermore, a positive lower bound of the trigger interval has been given to avoid Zeno behaviour, that is:

Theorem 3.2. *Let Assumption 2.1 hold, with suitable positive constants α_x^χ and β_x^χ, if the following equations are true:*

$$\Pi_x^R = \sum_{y=1}^{n}\left[-\sum_{k=1}^{q}\frac{a_{xk}}{l_k^2} - b_x - \alpha_x^R + \frac{1}{2}\hat{c}_{xy}^R l_y^R + \frac{1}{2}\hat{c}_{yx}^R l_x^R + \frac{1}{2}\hat{c}_{xy}^I l_y^I + \frac{1}{2}\hat{c}_{yx}^I l_x^R\right] < 0, \tag{23}$$

$$\Pi_x^I = \sum_{y=1}^{n}\left[-\sum_{k=1}^{q}\frac{a_{xk}}{l_k^2} - b_x - \alpha_x^I + \frac{1}{2}\hat{c}_{xy}^R l_y^I + \frac{1}{2}\hat{c}_{yx}^R l_x^I + \frac{1}{2}\hat{c}_{xy}^I l_y^R + \frac{1}{2}\hat{c}_{yx}^I l_x^I\right] < 0, \tag{24}$$

$$\begin{cases} sign\left(e_x^R\right) sign\left(e_x^R(t_k)\right) > 0, & \beta_x^R > P_x^R,\ \varpi = 1,\\ sign\left(e_x^R\right) sign\left(e_x^R(t_k)\right) \le 0, & \beta_x^R \le P_x^R,\ \varpi = -1, \end{cases} \tag{25}$$

and

$$\begin{cases} sign\left(e_x^I\right) sign\left(e_x^I\left(t_k\right)\right) > 0, & \beta_x^I > P_x^I,\ \varpi = 1, \\ sign\left(e_x^I\right) sign\left(e_x^I\left(t_k\right)\right) \le 0, & \beta_x^I \le P_x^I,\ \varpi = -1, \end{cases} \tag{26}$$

then the systems (4) and (18) can achieve exponential synchronization under the controller (21), and the event-triggered function satisfies

$$\Xi = \alpha_{\max}\left\|\hat{E}\right\|_1 \|E\|_1 + \rho\left(\Pi\|E\|_2^2 - \sum_{x=1}^{n}\left(\left|e_x^R\right| P_x^R + \left|e_x^I\right| P_x^I\right)\right), \tag{27}$$

where ρ *is an appropriate constant,* $E = \left(e_1^R, e_2^R, \ldots, e_n^R, e_1^I, e_2^I, \ldots, e_n^I\right)^T$, $1 > \alpha > 0$ *represents the order of the system,* $B = diag\left(b_1, b_2, \ldots, b_n\right)$, $\hat{E}(t_k) = \left(\hat{e}_1^R\left(t_k\right), \hat{e}_2^R\left(t_k\right), \ldots, \hat{e}_n^R(t_k), \hat{e}_1^I(t_k), \hat{e}_2^I\left(t_k\right), \ldots, \hat{e}_n^I(t_k)\right)^T$, $\Pi = \max\left\{\Pi_1, \Pi_2\right\}$, $\Pi_1 = \max\left\{\Pi_1^R, \Pi_2^R, \ldots, \Pi_n^R\right\}$, $\Pi_2 = \max\left\{\Pi_1^I, \Pi_2^I, \ldots, \Pi_n^I\right\}$, $L = 2\left(\left\|C^R\right\|_1 + \left\|D^R\right\|_1 + \left\|C^I\right\|_1 + \left\|D^I\right\|_1\right)\left(\left\|M^R\right\|_1 + \left\|M^I\right\|_1\right) + \left(\|B\|_1 + \left\|\alpha^R\right\|_1\right) \times \left\|E^R(t_k)\right\|_1 + \left(\|B\|_1 + \left\|\alpha^I\right\|_1\right)\left\|E^I(t_k)\right\|_1 + \sum_{x=1}^{n}\left|\beta_x^R\right| + \sum_{x=1}^{n}\left|\beta_x^I\right| + \sum_{x=1}^{n}\sum_{y=1}^{n}\left|\left(D_{xy}^R + D_{xy}^I\right)\dot{F}\right|$, *and* $C^\chi = \left(c_{xy}^{\chi+}\right)_{n\times n}$, $D^\chi = \left(d_{xy}^{\chi+}\right)_{n\times n}$, $M^\chi = \left(l_1^\chi, l_2^\chi, \ldots, l_n^\chi\right)^T$, $E^\chi(t_k) = \left(e_1^\chi(t_k), e_2^\chi(t_k), \ldots, e_n^\chi(t_k)\right)^T$, $P_x^R = \sum_{y=1}^{n}\left(\tilde{c}_{xy}^R G_y^R + \tilde{c}_{xy}^R G_y^I + \tilde{d}_{xy}^R G_y^R + \tilde{d}_{xy}^R G_y^I - \beta_x^R\right)$, $P_x^I = \sum_{y=1}^{n}\tilde{c}_{xy}^R G_y^I + \tilde{c}_{xy}^I G_y^R + \tilde{d}_{xy}^R G_y^I + \tilde{d}_{xy}^I G_y^R - \beta_x^I$, $\alpha_{\max}^R = \max_{x=1}^{n}\left\{\alpha_x^R\right\}$, $\alpha_{\max}^I = \max_{x=1}^{n}\left\{\alpha_x^I\right\}$, $\alpha_{\max}^R = \max_{x=1}^{n}\left\{\alpha_x^R\right\}$.

Moreover, the lower bound of the trigger interval time is obtained by

$$T_k \ge \left\{\frac{\Gamma(\alpha+1)}{\|B\|_1}\ln\left\{\frac{\|B\|_1 \ddagger}{\left[L + \left\|\hat{E}(t_k)\right\|_1\right]}\right\}\right\}^{\frac{1}{\alpha}}, \quad \hat{E}(t_0) = 0, \tag{28}$$

where

$$\ddagger = \left[\frac{\rho\left(\Pi\|E\|_2^2 + \sum_{x=1}^{n}\left|e_x^R\right| P_x^R + \sum_{x=1}^{n}\left|e_x^I\right| P_x^I\right)}{\alpha_{\max}\|E\|_1} + \frac{L}{\|B\|_1}\right].$$

Proof: Choose the following Lyapunov function:

$$V_2 = V_2^R + V_2^I, \tag{29}$$

where $V_2^\chi = \frac{1}{2}\int_\Omega \sum_{x=1}^{n}\left(e_x^\chi\right)^2 dz$.

Now, by calculating the α-derivative for $V_2^R(t)$ along (19), one has

$$\begin{aligned} D^\alpha V_2^R \le & \int_\Omega \sum_{x=1}^{n}\left(e_x^R\right)\left[\sum_{k=1}^{q}\frac{\partial}{\partial z_k}\left(a_{xk}\frac{\partial e_x^R}{\partial z_k}\right) - b_x e_x^R - \alpha_x^R e_x^R\right]dz \\ & + \int_\Omega \sum_{x=1}^{n}\sum_{y=1}^{n}\left|e_x^R\right|\left[\hat{c}_{xy}^R\left(l_y^R\left|e_y^R\right|\right) + \hat{c}_{xy}^I\left(l_y^I\left|e_y^I\right|\right)\right]dz \\ & + \int_\Omega \sum_{x=1}^{n}\sum_{y=1}^{n}\left|e_x^R\right|\left[\tilde{c}_{xy}^R G_y^R + \tilde{c}_{xy}^R G_y^I + \tilde{d}_{xy}^R G_y^R + \tilde{d}_{xy}^R G_y^I\right. \\ & \left. - \beta_x^R sign\left(e_x^R\right) sign\left(e_x^R\left(t_k\right)\right)\right]dz - \int_\Omega \sum_{x=1}^{n}\sum_{y=1}^{n}\alpha_x^R \hat{e}_x^R e_x^R dz \\ & + \int_\Omega \sum_{x=1}^{n}\sum_{y=1}^{n}\left|e_x^R\right|\left[D_{xy}^R\left(l_y^R\left|e_{y\sigma}^R\right|\right) + D_{xy}^I\left(l_y^I\left|e_{y\sigma}^I\right|\right)\right. \end{aligned}$$

$$- sign\left(e_x^R\right)\left[D_{xy}^R + D_{xy}^I\right]\varpi \dot{F} sign\left(e_x^R\left(t_k\right)\right)\Big] dz. \tag{30}$$

Moreover, by the fundamental inequality, it is obvious that

$$\begin{aligned}
&\sum_{x=1}^{n}\sum_{y=1}^{q}\left|e_x^R\right|\left[\hat{c}_{xy}^R l_y^R\left|e_y^R\right| + \hat{c}_{xy}^I l_y^I\left|e_y^I\right|\right] \\
&\leq \sum_{x=1}^{n}\sum_{y=1}^{q}\frac{1}{2}\hat{c}_{xy}^R l_y^R\left[\left(e_x^R\right)^2 + \left(e_y^R\right)^2\right] + \sum_{x=1}^{n}\sum_{y=1}^{q}\frac{1}{2}\hat{c}_{xy}^I l_y^I\left[\left(e_x^R\right)^2 + \left(e_y^I\right)^2\right].
\end{aligned} \tag{31}$$

Substitute Equations (13) and (31) into (30), and calculate $D^\alpha V_2^I$ in the same way, and then, combining with (23)-(26), one has

$$D^\alpha V_2 \leq \int_\Omega \left[\Pi\|E\|_2^2 + \sum_{x=1}^{n}\left|e_x^R\right| P_x^R dz + \sum_{x=1}^{n}\left|e_x^I\right| P_x^I dz - \alpha_{\max}\left\|\hat{E}\right\|_1 \|E\|_1\right] dz.$$

Moreover, from the event-triggered mechanism (27), we have

$$D^\alpha V_2(t) \leq \int_\Omega \sum_{x=1}^{n}\Pi_1\left(e_x^R\right)^2 + \sum_{x=1}^{n}\Pi_2\left(e_x^I\right)^2 \leq 2(1-\rho)\Pi V_2(t) < 0. \tag{32}$$

According to Lemma 2.4 in [48] and (32), it is easily obtained: $V_2(t) \leq V_2(0)e^{\frac{2(1-\rho)\Pi}{\Gamma(\alpha+1)}t^\alpha}$. Furthermore,

$$\|m(z,t) - s(z,t)\|_2 \leq \|\varphi - \phi\|_2 e^{\frac{(1-\rho)\Pi}{\Gamma(\alpha+1)}t^\alpha}. \tag{33}$$

Then, according to Definition 2.4, systems (4) and (18) achieve exponential synchronization with controller (21). This completes the proof. □

Now, a positive lower bound for the triggered interval time will be derived to avoid the Zeno behavior.

Step 1: From (22) and (27), for $t \in [t_k, t_{k+1})$, we have

$$\left\|\hat{E}\left(t_{k+1}\right)\right\|_1 \geq \rho\frac{\Pi\|E\|_2^2 + \sum_{x=1}^{n}\left|e_x^R\right| P_x^R + \sum_{x=1}^{n}\left|e_x^I\right| P_x^I}{\alpha_{\max}\|E\|_1}. \tag{34}$$

In addition, from the derivation of Theorem 3.2, we have

$$\begin{aligned}
\frac{\partial^\alpha\left\|\hat{E}\right\|_1}{\partial t^\alpha} &\leq \left\|\frac{\partial^\alpha \hat{E}}{\partial t^\alpha}\right\|_1 = \left\|\frac{\partial^\alpha E}{\partial t^\alpha}\right\|_1 \\
&\leq \|A\|_1\nabla\|E\|_1 + \|B\|_1\left\|\hat{E}\right\|_1 + 2\left(\left\|C^R\right\|_1 + \left\|D^R\right\|_1\right. \\
&\quad \left. + \left\|C^I\right\|_1 + \left\|D^I\right\|_1\right)\left(\left\|M^R\right\|_1 + \left\|M^I\right\|_1\right) \\
&\quad + \left(\|B\|_1 + \left\|\alpha^R\right\|_1\right)\left\|E^R(t_k)\right\|_1 + \left(\|B\|_1 + \left\|\alpha^I\right\|_1\right)\left\|E^I(t_k)\right\|_1 \\
&\quad + \sum_{x=1}^{n}\left|\beta_x^R\right| + \sum_{x=1}^{n}\left|\beta_x^I\right| + \sum_{x=1}^{n}\sum_{y=1}^{n}\left|\left(D_{xy}^R + D_{xy}^I\right)\dot{F}\right| \\
&\leq \|B\|_1\left\|\hat{E}(t)\right\|_1 + L.
\end{aligned} \tag{35}$$

Step 2: Constructing a variable substitution as $\left\|\hat{E}^*(t)\right\|_1 \triangleq \left\|\hat{E}(t)\right\|_1 + \frac{L}{\|B\|_1}$, such that

$$\frac{\partial^\alpha\left\|\hat{E}^*(t)\right\|_1}{\partial t^\alpha} \leq \|B\|_1\left(\left\|\hat{E}^*(t)\right\|_1 - \frac{L}{\|B\|_1}\right) + L = \|B\|_1\left\|\hat{E}^*(t)\right\|_1,$$

and then, there exists a real function $\Im(t)$ that

$$\frac{\partial^\alpha \left\|\hat{E}^*(t)\right\|_1}{\partial t^\alpha} = \|B\|_1 \left\|\hat{E}^*(t)\right\|_1 - \Im(t). \tag{36}$$

Step 3: Taking the α-order integral for both sides of (36), we have

$$\begin{aligned}\left\|\hat{E}^*(t)\right\|_1 &= \left\|\hat{E}^*(t_0)\right\|_1 - \int_{t_0}^{t} \frac{(t-\tau)^{\alpha-1}}{\Gamma(\alpha)} \left(-\|B\|_1 \left\|\hat{E}^*(\tau)\right\|_1 + \Im(t)\right) d\tau \\ &\leq \left\|\hat{E}^*(t_0)\right\|_1 + \frac{\|B\|_1}{\Gamma(\alpha)} \int_{t_0}^{t} (t-\tau)^{\alpha-1} \left\|\hat{E}^*(\tau)\right\|_1 d\tau,\end{aligned}$$

and then, according to Lemma 2.1, the following equation holds

$$\left\|\hat{E}^*(t)\right\|_1 \leq \left\|\hat{E}^*(t_0)\right\|_1 \exp\left(\frac{\|B\|_1 (t-t_0)^\alpha}{\Gamma(\alpha+1)}\right). \tag{37}$$

Step 4: By taking $\left\|\hat{E}^*(t)\right\|_1 \triangleq \left\|\hat{E}(t)\right\|_1 + \frac{L}{\|B\|_1}$ into (37), and when $\left\|\hat{E}(t_0)\right\|_1 = 0$ and $t \in [t_k, t_{k+1})$, one has

$$\left\|\hat{E}(t)\right\|_1 \leq \left(\left\|\hat{E}(t_k)\right\|_1 + \frac{L}{\|B\|_1}\right) \exp\left(\frac{\|B\|_1 (t-t_k)^\alpha}{\Gamma(\alpha+1)}\right) - \frac{L}{\|B\|_1},$$

and hence,

$$\begin{aligned}&\frac{\Pi\|E\|_2^2 + \int_\Omega \sum_{x=1}^n \left|e_x^R\right| P_x^R dz + \int_\Omega \sum_{x=1}^n \left|e_x^I\right| P_x^I dz}{\alpha_{\max}\|E\|_1} \\ &\leq \left(\left\|\hat{E}(t_k)\right\|_1 + \frac{L}{\|B\|_1}\right) \exp\left(\frac{\|B\|_1 (t-t_k)^\alpha}{\Gamma(\alpha+1)}\right) - \frac{L}{\|B\|_1}.\end{aligned} \tag{38}$$

Step 5: From (38), we can derive the positive lower bound of the triggered interval time, that

$$T_k \geq \left\{\frac{\Gamma(\alpha+1)}{\|B\|_1} \ln\left\{\frac{\|B\|_1 \ddagger}{\left[L + \left\|\hat{E}(t_k)\right\|_1\right]}\right\}\right\}^{\frac{1}{\alpha}}, \tag{39}$$

where

$$\ddagger = \left[\frac{\rho\left(\Pi\|E\|_2^2 + \sum_{x=1}^n \left|e_x^R\right| P_x^R + \sum_{x=1}^n \left|e_x^I\right| P_x^I\right)}{\alpha_{\max}\|E\|_1} + \frac{L}{\|B\|_1}\right].$$

This completes the proof. □

Remark 3.2. *It is well known that the event-triggered frequency has a direct relationship with the trigger threshold. As we can see from the event-triggered function (27), the factors affecting the trigger threshold include controller parameters α, system parameters Π, P_x^χ, system error $e(t)$, and parameter ρ. Among them, the parameter ρ can directly change the trigger threshold, moreover, compared with other factors, the value of ρ is the easiest to change in practice, so the event-triggered frequency can be controlled by changing ρ.*

4. **Simulation Studies.** In this section, we provide two numerical examples to support the feasibility of the results in this paper. One illustrates the FOCVNNs with reaction-diffusion terms are dissipative and the other shows that master-slave system (4) and (18) can achieve exponential synchronization under the event-triggered controller (21).

Example 4.1. *Construct the 3-dimensional FOCVNNs with reaction-diffusion terms for (4), where* $\alpha = 0.97$, $q = 1$, $n = 3$ *and the system parameters* $a_{11} = a_{21} = a_{31} = 0.02$, $b_1 = b_2 = b_3 = 25$, $\sigma(z,t) = \frac{e^t}{e^t+1}$, $O_1^R = 0.02$, $O_2^R = 0.01$, $O_3^R = -0.03$, $O_1^I = -0.02$, $O_2^I = -0.01$, $O_3^I = 0.03$, $\Upsilon_1^\chi = \Upsilon_2^\chi = \Upsilon_3^\chi = 0.9$, *and we choose the connection weights as Table 2, where* $\dagger = s(t)$. *Furthermore, we set* $\imath_k^2 = 2$, $g_y^R(\cdot) = 0.9\tanh(\cdot) + 0.02sign(\cdot)$, $g_y^I(\cdot) = 0.9\tanh(\cdot) + 0.01sign(\cdot)$ *as activation function, and the initial conditions for (4) are* $s_1^R(z,0) = -0.02\sin(z)$, $s_2^R(z,0) = 0.01\sin(z)$, $s_3^R(z,0) = 0.02\sin(z)$, $s_1^I(z,0) = -0.03 \times \sin(z)$, $s_2^I(z,o) = 0.04\sin(z)$, $s_3^I(z,o) = 0.02\sin(z)$, *with* $(z,o) \in \Omega \times [-0.953, 0]$.

TABLE 2. The connection weights for Example 4.1

$$c_{11}(\dagger) = \begin{cases} 1.1 + i0.5 & |\dagger| \le 0.9 \\ 1.3 + i0.9 & |\dagger| > 0.9 \end{cases} \quad c_{21}(\dagger) = \begin{cases} -0.9 + i0.4 & |\dagger| \le 0.9 \\ -0.6 + i0.7 & |\dagger| > 0.9 \end{cases}$$

$$c_{31}(\dagger) = \begin{cases} -0.8 - i0.2 & |\dagger| \le 0.9 \\ -0.6 - i0.4 & |\dagger| > 0.9 \end{cases} \quad c_{12}(\dagger) = \begin{cases} 0.7 - i0.4 & |\dagger| \le 0.9 \\ -0.1 - i0.1 & |\dagger| > 0.9 \end{cases}$$

$$c_{22}(\dagger) = \begin{cases} -0.6 + i0.7 & |\dagger| \le 0.9 \\ -0.4 + i0.5 & |\dagger| > 0.9 \end{cases} \quad c_{32}(\dagger) = \begin{cases} 0.6 + i0.7 & |\dagger| \le 0.9 \\ 0.8 + i0.3 & |\dagger| > 0.9 \end{cases}$$

$$c_{13}(\dagger) = \begin{cases} 0.7 - i0.6 & |\dagger| \le 0.9 \\ 0.8 - i0.4 & |\dagger| > 0.9 \end{cases} \quad c_{23}(\dagger) = \begin{cases} 0.7 - i0.8 & |\dagger| \le 0.9 \\ -0.5 - i0.6 & |\dagger| > 0.9 \end{cases}$$

$$c_{33}(\dagger) = \begin{cases} 0.5 - i0.6 & |\dagger| \le 0.9 \\ 0.7 - i0.8 & |\dagger| > 0.9 \end{cases} \quad d_{11}(\dagger) = \begin{cases} 0.6 + i0.5 & |\dagger| \le 0.9 \\ 0.5 + i0.1 & |\dagger| > 0.9 \end{cases}$$

$$d_{21}(\dagger) = \begin{cases} -0.5 + i0.5 & |\dagger| \le 0.9 \\ -0.2 - i0.2 & |\dagger| > 0.9 \end{cases} \quad d_{31}(\dagger) = \begin{cases} -0.4 - i0.1 & |\dagger| \le 0.9 \\ -0.5 + i0.4 & |\dagger| > 0.9 \end{cases}$$

$$d_{12}(\dagger) = \begin{cases} -0.2 - i0.3 & |\dagger| \le 0.9 \\ -0.5 + i0.2 & |\dagger| > 0.9 \end{cases} \quad d_{22}(\dagger) = \begin{cases} 0.2 + i0.2 & |\dagger| \le 0.9 \\ 0.4 + i0.6 & |\dagger| > 0.9 \end{cases}$$

$$d_{32}(\dagger) = \begin{cases} 0.5 - i0.3 & |\dagger| \le 0.9 \\ 0.3 - i0.2 & |\dagger| > 0.9 \end{cases} \quad d_{13}(\dagger) = \begin{cases} 0.4 - i0.2 & |\dagger| \le 0.9 \\ 0.3 - i0.3 & |\dagger| > 0.9 \end{cases}$$

$$d_{23}(\dagger) = \begin{cases} -0.6 - i0.3 & |\dagger| \le 0.9 \\ -0.4 - i0.3 & |\dagger| > 0.9 \end{cases} \quad d_{33}(\dagger) = \begin{cases} 0.4 + i0.4 & |\dagger| \le 0.9 \\ 0.9 - i0.4 & |\dagger| > 0.9 \end{cases}$$

Now, we can calculate $M + N = -182.18 < 0$, $W = 0.0028$ *and the dissipative set* $B(0, 0.01)$ *with* $\varepsilon = 0.0061$. *Therefore, based on Theorem 3.1, the system (4) can achieve global dissipative which is shown in Figure 1.*

Example 4.2. *In this example, a 2-dimensional model is constructed with* $\alpha = 0.97$, $a_{11} = a_{21} = 0.01$, $b_1 = b_2 = 2$, $n = 2$, *and the connection weights are chosen as*

$$c_{11}(\aleph) = \begin{cases} 1.2 + i0.2 & |\aleph| \le 0.9, \\ 0.5 + i0.3 & |\aleph| > 0.9, \end{cases} \quad c_{12}(\aleph) = \begin{cases} 0.8 - i0.3 & |\aleph| \le 0.9, \\ -1.2 - i0.6 & |\aleph| > 0.9, \end{cases}$$

$$c_{21}(\aleph) = \begin{cases} -1.1 + i0.4 & |\aleph| \le 0.9, \\ 0.8 + i0.9 & |\aleph| > 0.9, \end{cases} \quad c_{22}(\aleph) = \begin{cases} -0.7 + i0.6 & |\aleph| \le 0.9, \\ 0.4 + i0.7 & |\aleph| > 0.9, \end{cases}$$

$$d_{11}(\aleph) = \begin{cases} 0.6 + i0.3 & |\aleph| \le 0.9, \\ 0.5 + i0.5 & |\aleph| > 0.9, \end{cases} \quad d_{12}(\aleph) = \begin{cases} -0.4 - i0.2 & |\aleph| \le 0.9, \\ 0.5 + i0.3 & |\aleph| > 0.9, \end{cases}$$

$$d_{21}(\aleph) = \begin{cases} -0.3 + i0.2 & |\aleph| \le 0.9, \\ 0.5 + i0.3 & |\aleph| > 0.9, \end{cases} \qquad d_{22}(\aleph) = \begin{cases} 0.2 + i0.4 & |\aleph| \le 0.9, \\ -0.4 + i0.2 & |\aleph| > 0.9, \end{cases}$$

where $\aleph = (s(t), m(t))$, *and the initial condition is selected as* $s_1^R(z,0) = -1.2\sin(z)$, $s_2^R(z,0) = 1.4\sin(z)$, $s_1^I(z,0) = -1.6\sin(z)$, $s_2^I(z,o) = 1.8\sin(z)$, $m_1^R(z,0) = 1.7\sin(z)$, $m_2^R(z,0) = -2.5\sin(z)$, $m_1^I(z,0) = 1.8\sin(z)$, $m_2^I(z,o) = -1.1\sin(z)$.

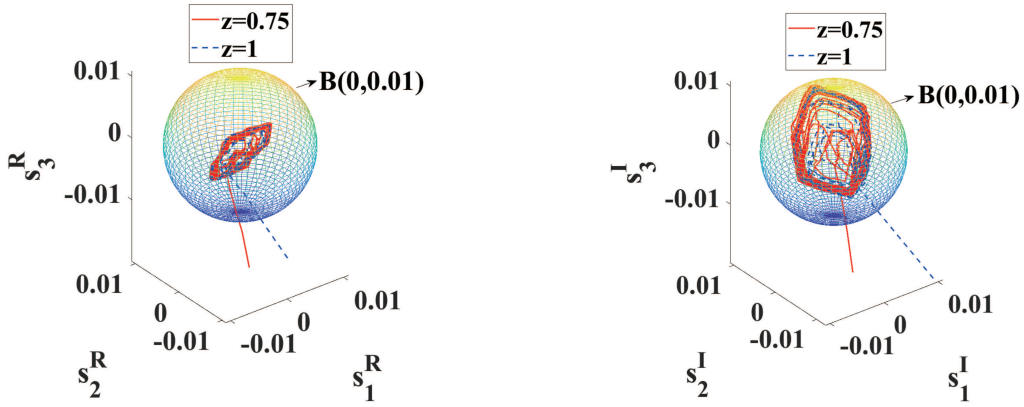

FIGURE 1. Phase diagram of system (5): (a) Real part; (b) imaginary part

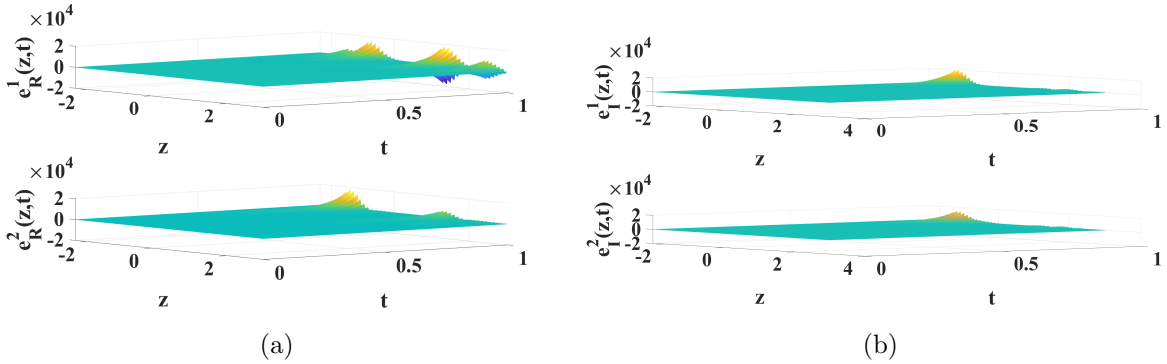

FIGURE 2. The synchronization error state without controller: (a) $e^R(z,t)$; (b) $e^I(z,t)$

The other parameters are the same as in Example 4.1, and then the error state trajectories without controller are shown in Figure 2. In addition, the controller parameters are designed as $\alpha_1^R = 2$, $\alpha_1^I = 3$, $\alpha_2^R = 3$, $\alpha_2^I = 3.5$, $\beta_1^R = 4.5$, $\beta_1^I = 3$, $\beta_2^R = 2.5$, $\beta_2^I = 1.5$, *and then, the synchronization error and the trigger interval of the considered system under the event-triggered mechanism (22) are shown in Figures 3-6 with* $\rho = 0.02$ *and* $\rho = 0.05$, *respectively. From Figures 3 and 5, it can be seen that the synchronization error can converge to zero under the event-triggered function (27) with* $\rho = 0.02$ *and* $\rho = 0.05$, *respectively. Moreover, Figures 4 and 6 show the event-triggered frequency at* $z = 1.5$ *and* $z = 4.5$, *respectively.*

Furthermore, to exhibit the role of ρ in the controller. Tables 3 and 4 are given, where N_t indicates the number of triggers; A_i is the average release interval and C_t is the controller data transfer rate, respectively.

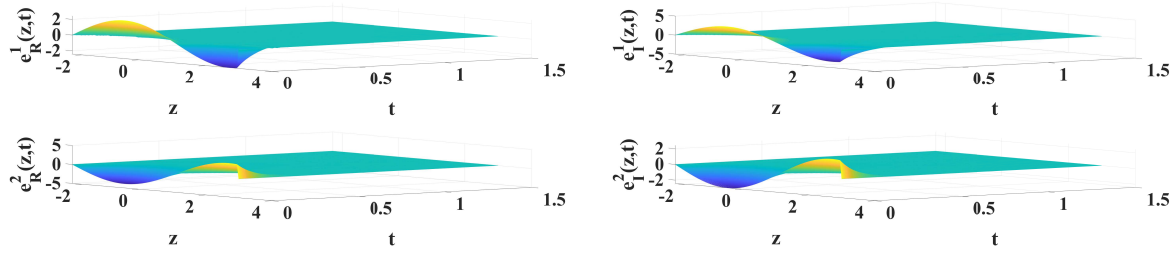

(a) (b)

FIGURE 3. The synchronization error state with controller and $\rho = 0.02$: (a) $e^R(z,t)$; (b) $e^I(z,t)$

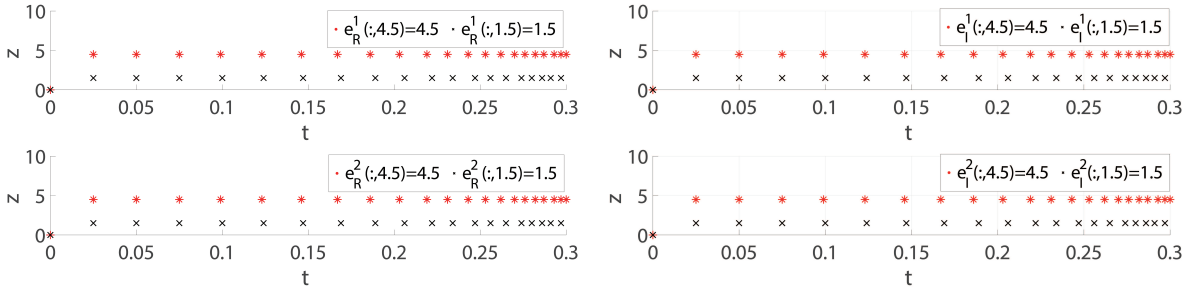

(a) (b)

FIGURE 4. The instantaneous moment of triggering with $\rho = 0.02$: (a) $e^R(z,t)$; (b) $e^I(z,t)$

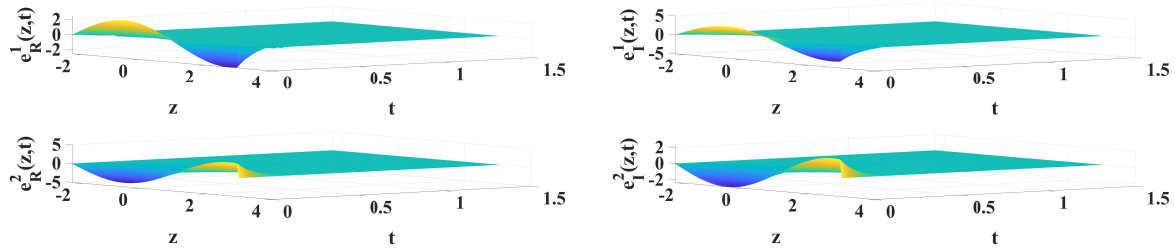

(a) (b)

FIGURE 5. The error state trajectory with controller and $\rho = 0.05$: (a) $e^R(z,t)$; (b) $e^I(z,t)$

As can be seen from Tables 3 and 4, when $\rho = 0$, the system does not reduce the communication frequency, i.e., the event-triggered mechanism is ineffective. Furthermore, with the value of ρ increase, the triggered frequency gradually decreases, which indicates that the controller is effective. It is worth noting that when $\rho > 0.1$, the event-triggered mechanism will be difficult to be satisfied, which means that the triggered frequency is reduced and the controller is ineffective.

Remark 4.1. *According to event-triggered function (27), the triggering threshold will be smaller when the system achieves stable. Moreover, the error system will oscillate around 0 due to the presence of the sign function in the controller, which means that the triggering will occur frequently. To avoid this phenomenon, in practice, the tanh function is used*

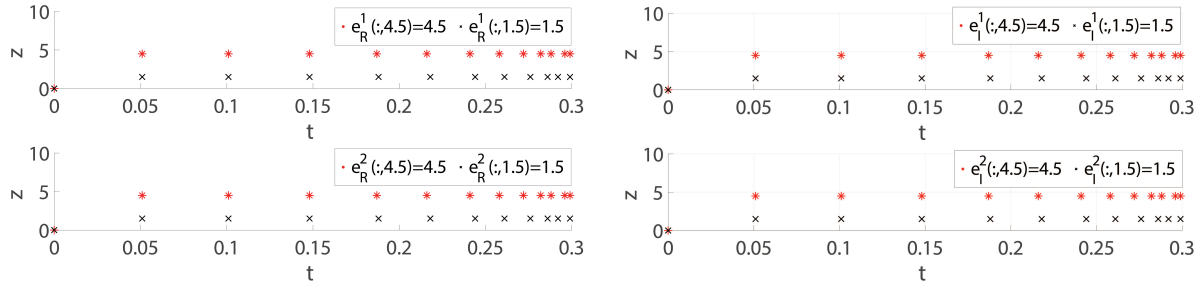

(a) (b)

FIGURE 6. The instantaneous moment of triggering with $\rho = 0.05$: (a) $e^R(z,t)$; (b) $e^I(z,t)$

TABLE 3. The real-valued part

ρ	0	0.01	0.02	0.04	0.06	0.1
N_t	300	37	21	12	9	7
A_i	0.001	0.008	0.014	0.025	0.033	0.043
C_t	100%	12.33%	7%	4%	3%	2.33%

TABLE 4. The complex-valued part

ρ	0	0.01	0.02	0.04	0.06	0.1
N_t	300	36	20	12	8	6
A_i	0.001	0.008	0.015	0.025	0.0375	0.05
C_t	100%	12.00%	6.67%	4.00%	2.67%	2.00%

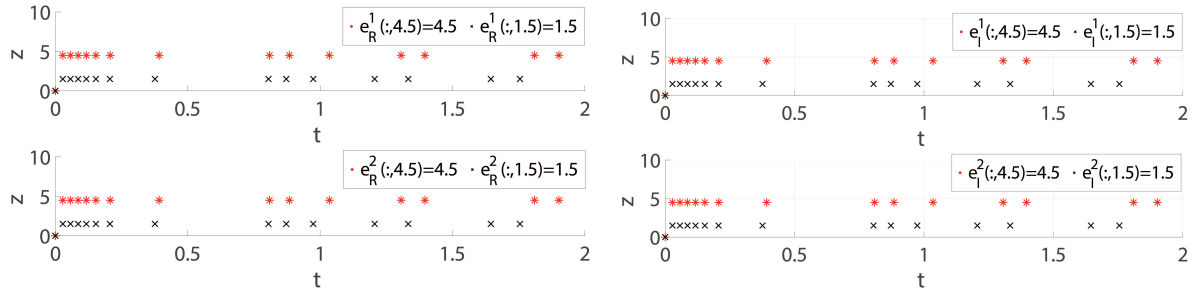

(a) (b)

FIGURE 7. The instantaneous moment of triggering with $\rho = 0.02$ (using the tanh function instead of the sign function): (a) $e^R(z,t)$; (b) $e^I(z,t)$

instead of the sign one. Specially, it can be seen from Figure 7 that the triggering frequency decreases significantly after stabilization.

5. **Conclusion.** In this paper, the dissipative and event-triggered exponential synchronization of a class of FOCVNNs with reaction-diffusion terms has been investigated. First, we have proved that the FOCVNNs with reaction-diffusion terms were globally dissipative via the fractional Halanay inequality. In addition, a new event-triggered controller has been designed to reduce the communication bandwidth, and the FOCVNNs with reaction-diffusion terms were demonstrated to be exponentially synchronization via the

event-triggered mechanism. Furthermore, a positive lower bound on the trigger interval time have been given to avoid the Zeno behavior. Finally, two numerical examples have proved to verify the results of this paper.

Acknowledgements. This work was supported in part by the National Natural Science Foundation of China under Grant 61976081, in part by the Natural Science Fund for Excellent Young Scholars of Henan Province under Grant 202300410127, and in part by Key Scientific Research Projects of Higher Education Institutions in Henan Province under Grant 22A413001.

REFERENCES

[1] A. Goltsev and V. Gritsenko, Investigation of efficient features for image recognition by neural networks, *Neural Networks*, vol.28, pp.15-23, 2012.
[2] Z. Dong, X. Zhang and X. Wang, State estimation for discrete-time high-order neural networks with time-varying delays, *Neurocomputing*, vol.411, pp.282-290, 2020.
[3] F. Ponulak and A. Kasinski, Introduction to spiking neural networks: Information processing, learning and applications, *Acta Neurobiologiae Experimentalis*, vol.71, no.4, pp.409-433, 2011.
[4] M. Xue, Y. Tang, W. Ren and F. Qian, Practical output synchronization for asynchronously switched multi-agent systems with adaption to fast-switching perturbations, *Automatica*, vol.116, DOI: 10.1016/j.automatica.2020.108917, 2020.
[5] Y. Xu, J. Li, R. Lu, C. Liu and Y. Wu, Finite-horizon l_2-l_∞ synchronization for time-varying Markovian jump neural networks under mixed-type attacks: Observer-based case, *IEEE Trans. Neural Networks and Learning Systems*, vol.30, no.6, pp.1695-1704, 2019.
[6] J. Hu, Z. Wang, S. Liu and H. Gao, A variance-constrained approach to recursive state estimation for time-varying complex networks with missing measurements, *Automatica*, vol.64, pp.155-162, 2016.
[7] F. Li, S. Song, J. Zhao, S. Xu and Z. Zhang, Synchronization control for Markov jump neural networks subject to HMM observation and partially known detection probabilities, *Applied Mathematics and Computation*, vol.360, pp.1-13, 2019.
[8] Y. Wang, W. Yang, J. Xiao and Z. Zeng, Impulsive multi synchronization of coupled multistable neural networks with time-varying delay, *IEEE Trans. Neural Networks and Learning Systems*, vol.28, no.7, pp.1560-1571, 2017.
[9] R. Xu, Anti-periodic dynamics in delayed neural networks with unidirectional coupling, *International Journal of Innovative Computing, Information and Control*, vol.15, no.1, pp.247-259, 2019.
[10] C. Lee and B.-D. Lee, Enhancement for automatic extraction of RoIs for bone age assessment based on deep neural networks, *ICIC Express Letters*, vol.14, no.2, pp.163-170, 2020.
[11] A. Boroomand and M. B. Menhaj, Fractional-order Hopfield neural networks, *Advances in Neuro-Information Processing*, vol.5506, no.1, pp.883-890, 2009.
[12] H. Bao and J. Cao, Projective synchronization of fractional-order memristor-based neural networks, *Neural Networks*, vol.63, pp.1-9, 2015.
[13] R. Wu, X. Hei and L. Chen, Finite-time stability of fractional-order neural networks with delay, *Communications in Theoretical Physics*, vol.60, no.2, pp.189-193, 2013.
[14] F. Wang, Y. Yang and M. Hu, Asymptotic stability of delayed fractional-order neural networks with impulsive effects, *Neurocomputing*, vol.154, no.22, pp.239-244, 2015.
[15] Z. Wu, P. Shi, H. Su and J. Chu, Dissipativity analysis for discrete-time stochastic neural networks with time-varying delays, *IEEE Trans. Neural Networks and Learning Systems*, vol.24, no.3, pp.345-355, 2013.
[16] D. Xu and Z. Yang, Dissipativity analysis for discrete-time stochastic neural networks with time-varying delays, *Journal of Mathematical Analysis and Applications*, vol.305, no.1, pp.107-120, 2005.
[17] J. Man, X. Song and J. Lu, Nonfragile memory-based output feedback control for fuzzy Markov jump generalized neural networks with reaction-diffusion terms, *International Journal of Innovative Computing, Information and Control*, vol.15, no.5, pp.1609-1628, 2019.
[18] X. Song, J. Man, J. H. Park and S. Song, Finite-time synchronization of reaction-diffusion inertial memristive neural networks via gain-scheduled pinning control, *IEEE Trans. Neural Networks and Learning Systems*, DOI: 10.1109/TNNLS.2021.3068734, 2021.
[19] K. Wu, M. Ren and X. Liu, Exponential input-to-state stability of stochastic delay reaction-diffusion neural networks, *Neurocomputing*, vol.412, pp.399-405, 2020.

[20] B. Zhou and Q. Song, Boundedness and complete stability of complex-valued neural networks with time delay, *IEEE Trans. Neural Networks and Learning Systems*, vol.24, no.8, pp.1227-1238, 2013.
[21] R. Rakkiyappan, J. Cao and G. Velmurugan, Existence and uniform stability analysis of fractional-order complex-valued neural networks with time delays, *IEEE Trans. Neural Networks and Learning Systems*, vol.26, no.1, pp.84-97, 2015.
[22] T. Nitta, Solving the XOR problem and the detection of symmetry using a single complex-valued neuron, *Neural Networks*, vol.16, no.8, pp.1101-1105, 2003.
[23] D. Wang, L. Huang and L. Tang, Synchronization criteria for discontinuous neural networks with mixed delays via functional differential inclusions, *IEEE Trans. Neural Networks and Learning Systems*, vol.29, no.5, pp.1809-1821, 2018.
[24] J. Chen, C. Li and X. Yang, Global Mittag-Leffler projective synchronization of nonidentical fractional-order neural networks with delay via sliding mode control, *Neurocomputing*, vol.313, pp.324-332, 2018.
[25] J. C. Willems, Dissipative dynamical systems part I: General theory, *Archive for Rational Mechanics and Analysis*, vol.45, no.5, pp.321-351, 1972.
[26] H. Shen, Y. Zhu, L. Zhang and J. H. Park, Extended dissipative state estimation for Markov jump neural networks with unreliable links, *IEEE Trans. Neural Networks and Learning Systems*, vol.28, no.2, pp.346-358, 2016.
[27] T. Wang, B. Zhang, D. Yuan and Y. Zhang, Event-based extended dissipative state estimation for memristor-based Markovian neural networks with hybrid time-varying delays, *IEEE Trans. Circuits and Systems I: Regular Papers*, DOI: 10.1109/TCSI.2021.3077485, 2021.
[28] K. Mathiyalagan, J. H. Park and R. Sakthivel, Synchronization for delayed memristive bam neural networks using impulsive control with random nonlinearities, *Applied Mathematics and Computation*, vol.259, no.15, pp.967-979, 2015.
[29] Y. Guo, Globally robust stability analysis for stochastic Cohen-Grossberg neural networks with impulse control and time-varying delays, *Ukrainian Mathematical Journal*, vol.69, no.6, pp.1220-1233, 2018.
[30] Z. Ning, K. Yu and C. Ming, Neural network-based adaptive control for spacecraft under actuator failures and input saturations, *IEEE Trans. Neural Networks and Learning Systems*, vol.31, no.9, pp.3696-3710, 2020.
[31] H. Liu, S. Li, J. Cao, G. Li, A. Alsaedi and F. E. Alsaadi, Adaptive fuzzy prescribed performance controller design for a class of uncertain fractional-order nonlinear systems with external disturbances, *Neurocomputing*, vol.219, no.5, pp.422-430, 2017.
[32] T. C. Lin, Based on interval type-2 fuzzy-neural network direct adaptive sliding mode control for SISO nonlinear systems, *Communications in Nonlinear Science and Numerical Simulation*, vol.15, no.12, pp.4084-4099, 2010.
[33] Z. Yan, X. Huang and J. Cao, Variable-sampling-period dependent global stabilization of delayed memristive neural networks based on refined switching event-triggered control, *Science China Information Sciences*, vol.63, no.11, pp.1-16, 2020.
[34] D. Zeng, R. Zhang, J. H. Park, Z. Pu and Y. Liu, Pinning synchronization of directed coupled reaction-diffusion neural networks with sampled-data communications, *IEEE Trans. Neural Networks and Learning Systems*, vol.31, no.6, pp.2092-2103, 2020.
[35] X. Li, W. Zhang, J. Fang and H. Li, Event-triggered exponential synchronization for complex-valued memristive neural networks with time-varying delays, *IEEE Trans. Neural Networks and Learning Systems*, vol.31, no.10, pp.4104-4116, 2020.
[36] S. Yang, J. Yu, C. Hu and H. Jiang, Quasi-projective synchronization of fractional-order complex-valued recurrent neural networks, *Neural Networks*, vol.104, pp.104-113, 2018.
[37] G. Velmurugan, R. Rakkiyappan, V. Vembarasan, J. Cao and A. Alsaedi, Dissipativity and stability analysis of fractional-order complex-valued neural networks with time delay, *Neural Networks*, vol.86, pp.42-53, 2017.
[38] Y. Huang, J. Hou and E. Yang, Passivity and synchronization of coupled reaction-diffusion complex-valued memristive neural networks, *Applied Mathematics and Computation*, vol.379, no.15, DOI: 10.1016/j.amc.2020.125271, 2020.
[39] Z. Tu, N. Ding, L. Li, Y. Feng, L. Zou and W. Zhang, Adaptive synchronization of memristive neural networks with time-varying delays and reaction-diffusion term, *Applied Mathematics and Computation*, vol.311, no.15, pp.118-128, 2017.

[40] X. Song, J. Man, S. Song and Z. Ning, Event-triggered synchronization of Markovian reaction-diffusion inertial neural networks and its application in image encryption, *IET Control Theory & Applications*, vol.14, no.18, pp.2726-2740, 2020.
[41] X. Wang, J. H. Park, S. Zhong and H. Yang, A switched operation approach to sampled-data control stabilization of fuzzy memristive neural networks with time-varying delay, *IEEE Trans. Neural Networks and Learning Systems*, vol.31, no.3, pp.891-900, 2020.
[42] J. J. E. Slotine and W. Li, *Applied Nonlinear Control*, Prentice Hall, Englewood Cliffs, 1991.
[43] I. Podlubny, *Fractional Differential Equations*, Academic Press, New York, NY, USA, 1999.
[44] C. W. Wu, *Synchronization in Complex Networks of Nonlinear Dynamical Systems*, World Scientific, Singapore, 2007.
[45] J. Lu, Global exponential stability and periodicity of reaction-diffusion delayed recurrent neural networks with Dirichlet boundary conditions, *Chaos, Solitons & Fractals*, vol.35, no.1, pp.116-125, 2008.
[46] D. Wang, A. Xiao and H. Liu, Dissipativity and stability analysis for fractional functional differential equations, *Fractional Calculus and Applied Analysis*, vol.18, no.6, pp.1399-1422, 2015.
[47] X. Liao and J. Wang, Global dissipativity of continuous-time recurrent neural networks with time delay, *Physical Review E*, vol.68, no.1, DOI: 10.1103/PhysRevE.68.016118, 2003.
[48] W. Li, X. Gao and R. Li, Dissipativity and synchronization control of fractional-order memristive neural networks with reaction-diffusion terms, *Mathematical Methods in the Applied Sciences*, vol.42, no.18, pp.7494-7505, 2019.

Author Biography

Xiangliang Sun received the B.S. degree in Measurement and Control Technology and Instrument from the School of Information Engineering, Pingdingshan University, Pingdingshan, China, in 2019. He is studying for the M.S. degree in the School of Information Engineering, Henan University of Science and Technology, Luoyang, China. His current research interests include fractional-order neural networks, multiagent systems and distributed parameter systems.

Xiaona Song received the Ph.D. degree in Control Theory and Control Engineering from Nanjing University of Science and Technology, Nanjing, China, in 2011. From Feb. 2009 to Aug. 2009 and Apr. 2016 to Apr. 2017, she was a visiting scholar with the Department of Electrical Engineering, Utah State University and Southern Illinois University Carbondale, respectively. Since 2011, she has been with Henan University of Science and Technology, Luoyang, China, where she is currently a Professor with the School of Information Engineering. Her current research interests include Markov jump distributed parameter systems, complex networks, fractional-order systems and control, fuzzy control, nonlinear control.